Sensitivity Analysis of Insulation State Indicator in Dependence of Sampling Rate and Bit Resolution to Define Hardware Requirements

P. Nussbaumer, Th.M. Wolbank
Institute of Energy Systems and Electrical Drives
Vienna University of Technology
Vienna, Austria
thomas.wolbank@tuwien.ac.at

M.A. Vogelsberger
Drives Development Center 1, PPC
Bombardier Transportation Austria GmbH
Vienna, Austria
markus.vogelsberger@at.transport.bombardier.com

***Abstract*—Industrial application of adjustable speed drives (ASD) has been constantly growing in the last decades. In addition to the sheer number of inverter-fed drives the variety of application fields is increasing too. The use of such ASD in safety critical devices or industrial systems with many drives installed leads to the requirement of increased reliability. Furthermore many drives are operated at or near their rated values to increase efficiency and return on investment. In comparison to mains-fed machines, high dynamics and the fast switching of the inverter adds significant stress to different components of inverter-fed drives. The electrical machine is one of the most important components in these drives. A major cause for machine breakdown is insulation related fault. It is important to mention that such faults do not occur suddenly but origin in an alteration of the insulation condition and finally lead to short circuits. This alteration of the insulation leads to changes in the machine's high-frequency (hf) behavior. To reduce the number of breakdowns and apply predictive maintenance insulation monitoring can be implemented.**

Monitoring of the machine's hf-behavior can be used to assess the insulation condition by investigation of the transients in the current or voltage. Thus oversampling of the sensor signals is needed. The needed sampling rate and resolution to detect alterations in the machine's hf-behavior is investigated by experimental results.

Keywords— AC motor drives, Fault diagnosis, Induction motor protection, Monitoring, Pulse width modulated inverters, Rotating machine insulation testing, Squirrel cage motors

I. INTRODUCTION

More and more variable speed drives are used due to their advantages according to flexibility and high dynamic torque/speed properties. Especially if used in safety-critical devices (e.g. in the "more electric aircraft") or in industrial production lines where outage of a single drive may lead to high economic losses, high reliability is a necessity. This requirement can be met with fault tolerant operation, preventive maintenance and continuous condition monitoring.

According to [1] and [2] stator related faults are with 35% the second most common faults that lead to machine breakdown. About 70% of these stator related faults are due to failure in the machine's insulation system that lead to short circuits.

Breakdown of the insulation system is usually a slowly developing process starting with degradation of the insulation material leading to a turn-to-turn fault that speeds up and finally results in a severe ground fault [3]. The major cause for insulation degradation is thermal strain [4]. However, electrical, mechanical and environmental stress may also influence this process. For electrical machines in inverter-fed drives the insulation system suffers from additional stress due to the fast switching of the inverter and the mismatch of cable and machine impedance leading to high overvoltage [3].

The detection of insulation faults and/or degradation has been extensively dealt with in literature. All developed methods can be classified to online or offline techniques.

The most common and industrially accepted monitoring methods are offline techniques. The DC conductivity [5], the insulation resistance (IR) [6], DC/AC HiPot [7], polarization index (PI) [7] and offline surge test [8] are some examples all summarized in [7].

A well known online insulation monitoring technique is the partial discharge (PD) test. This test, however, is only applicable for medium to high voltage machines [9]. Furthermore additional sensors and high sophisticated evaluation algorithms are needed.

Various other online techniques have been proposed and studied in literature. This introduction will not give a complete overview of all developed condition monitoring technique as this is not scope of the paper. However, a short selection will be presented in the following. Motor current signature analysis (MCSA) can be applied to detect turn faults [10], [11]. A variation of the surge test for online applicability has been developed in [12]. The phase-to-ground insulation can be monitored by measuring the leakage current from conductor to ground as presented in [3]. This monitoring method can be applied to inverter-fed machines also. The detection of a winding fault can be realized by measuring the current's reaction to voltage pulses applied by the voltage source inverter (VSI) as discussed in [14].

The following requirements have been defined as boundary conditions for the development of the monitoring technique used in this paper. No disassembling of the drive should be necessary. The method should be applicable for machines in

voltage source inverter-fed drives and no additional sensors should be needed. Furthermore, insulation degradation before a short circuit actually develops should be detectable.

Degradation of the insulation leads to a change in the machine's high-frequency behavior as investigated in [15]. The method is based on detecting these changes by evaluating the transient reaction of the phase current on fast inverter switching. To calculate the characteristic properties of the transient signal ringing visible in the phase current the signal has to be sampled with sufficient resolution in time. The influence of sampling time and bit resolution on the calculated insulation state indicator is investigated and evaluated by experimental results.

II. The Proposed Monitoring Technique – Fundamentals and General Aspects

If the machine's high-frequency behavior is taken into account too, the whole drive system forms a very complex impedance system consisting of the characteristic electrical parameters like stator resistance r_S and inductance l_S and the cables' resistance and inductance per unit length. Moreover the parasitic components like the machine's capacitances winding-to-ground, winding-to-winding and turn-to-turn, the cables' capacitive coupling to ground and the inverter's capacitance between power electronics and heat sink all influence the drive systems' electrical high frequency properties. The machine's and cables' insulation system define many of the above mentioned parasitic parameters. All these parameters are responsible for the mismatch between cable and machine impedance. According to signals and systems theory this impedance mismatch in combination with fast switching of the inverter's IGBTs lead to reflection of the voltage wave at the machine terminals. This results in an oscillating transient overvoltage with decaying amplitude superimposed to the actually applied voltage. The frequency of this oscillation is in the range of several hundred kHz to MHz as analyzed in [13] for example. However, this signal ringing is not only visible in the voltage but also in the current signal. The usage of phase current sensors for the evaluation of the insulation condition is advantageous as these sensors are usually already available in modern inverter-fed drive systems. A change of the machine's high-frequency behavior leads to a change in this high-frequency oscillation. The condition monitoring technique investigated is based on the analysis of these changes by evaluating the current's hf-oscillation with sufficient resolution in time.

III. Signal Processing and Measurement Procedure

As mentioned before the proposed monitoring procedure is based on detecting changes in the machine's high-frequency behavior. Thus the machine has to be excited in this frequency range. For voltage source inverter-fed drives this can be done by a simple change of the switching state as the rate of voltage rise is very high for modern drive systems. Immediately after the switching instant a decaying high-frequency ringing is detectable in the voltage and the phase current signal. The characteristic of this ringing is determined by the machine's high-frequency behavior that also depends on the health status of the insulation system and the high-frequency properties of the other drive components.

The chosen switching states in this investigation are from lower short circuit (000) to the active switching states +U (001), +V (010) or +W (100). The measured signal is the phase current during this switching transition and standard industrial current sensors can be used. The sampling rate of the analog-to-digital converters (ADC) has to be high enough to accurately resolve the characteristic frequencies in the investigated signal. The correct choice of the sampling rate is a crucial task and one of the main focuses in this paper.

Fig. 1 shows the typical current reaction during the described switching transition from lower short circuit to +U. The time instant of the switching transition is marked with a red arrow.

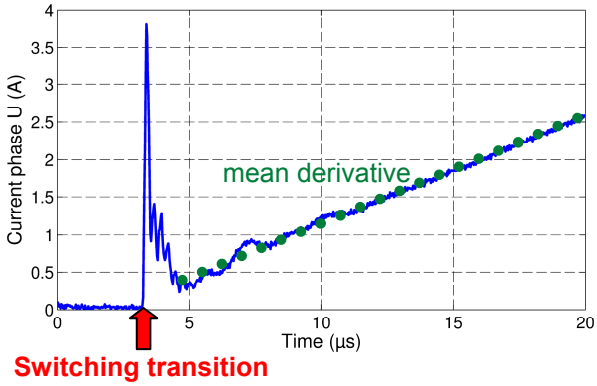

Fig. 1. Current signal with illustrated mean derivative (green, dotted line) and switching instant (red arrow).

The machine's transient reactance determines the derivative of the current after the transient signal ringing (further denoted as mean derivative) depicted as green, dotted line in Fig. 1. The transient reactance depends on the machine's inherent asymmetries e.g. due to slotting or saturation. Thus it is modulated depending on rotor and flux position. This dependency has to be eliminated by subtraction of the mean derivative (green, dotted line) of the respective acquired current signal.

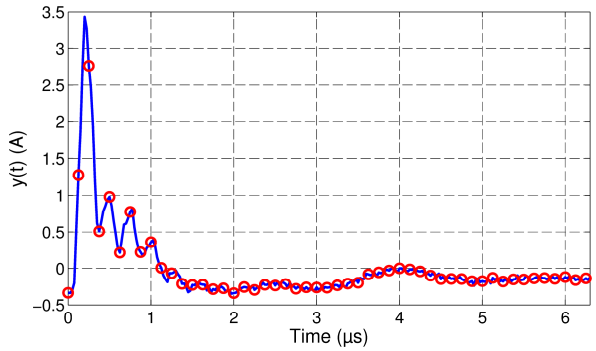

Fig. 2. Current (mean derivative subtracted) after switching transition from lower short circuit (000) to +U (001).

The investigated time window is chosen to the time span beginning with the actual switching instant detected by a triggering algorithm and ending after 6.4µs. For a sampling frequency of 40MS/s this equals N=256 values. The end is chosen constant. After this time the high-frequency ringing has decayed. The current after signal processing is depicted in Fig.

2. The exemplary sampling instants are highlighted with red circles.

The signal could be used as a reference if recorded for healthy machine condition and compared to later measurements (condition measurements). However, better results can be achieved if the signal in the frequency domain is chosen. Thus the signal is transformed to the frequency domain by fast Fourier transform (FFT). The amplitude spectrum of the signal in Fig. 2 is depicted in Fig. 3.

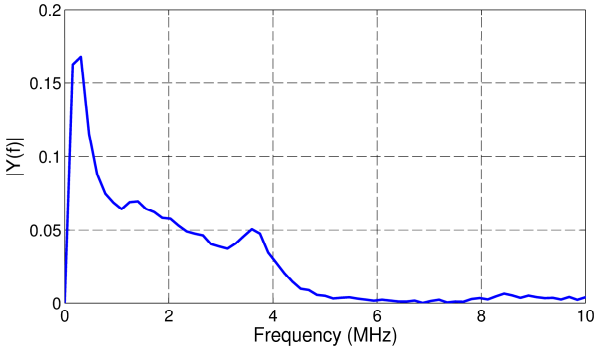

Fig. 3. Amplitude spectrum of measured current in phase U after switching transition from lower short circuit (000) to +U (001).

This amplitude spectrum serves as the reference trace for monitoring of phase U and is compared to all later measurements to assess the insulation condition. To detect changes of the machine's high-frequency behavior the measurement procedure and signal processing as described above is repeated for all other phases. After identification of the healthy machine an amplitude spectrum for each phase serving as reference trace exists, respectively. The measurement procedure and signal processing can be repeated whenever an assessment of the insulation condition is needed.

IV. Calculation of Insulation State Indicator

In the previous section the measurement procedure and signal processing that finally leads to an amplitude spectrum was described. To detect changes in the machine's high-frequency behavior the amplitude spectrum recorded for healthy machine condition is compared to all later measurements. To quantify the degree of change a comparative value is chosen as Insulation State Indicator (ISI). This indicator is calculated for each phase. The chosen comparative value is the root mean square deviation (RMSD) and is calculated as follows

$$ISI_{p,k} = RMSD_{p,k}(x_1, x_2) = \frac{\sqrt{\sum_{i=1}^{n}\left(Y_{ref,p}(i) - \left|Y_{con,p,k}(i)\right|\right)^2}}{n}. \quad (1)$$

The functions Y_{ref} and Y_{con} represent the amplitude spectrum of the reference and a later condition measurement, respectively. The index p (U,V,W) identifies the investigated phase. Here is to say that the switching transition as well as the measurement and signal processing are carried out for the corresponding phase. To increase the accuracy not only one but m measurements are taken into account. The amplitude spectrum is calculated for each measurement. In case of the healthy condition the mean trace of the amplitude spectrum serves as reference spectrum Y_{ref}. This amplitude spectrum is then compared to all m condition measurements. The index k marks the number of the consecutive measurements. In this investigation m is chosen to 140. The variable n depends on the frequency resolution and time window length. After the calculations according to (1) m comparative values exist for each phase. For a better understanding of the described comparison and calculations Fig. 4 shows the traces of the reference amplitude spectrum (blue, solid), a condition measurement with altered hf-behavior (1nF capacitor added in parallel to full phase winding U; blue, dashed) and the square deviation for the two blue traces. It can be easily discovered that the frequency spectrum is significantly altered in a small frequency range around 500kHz only. Thus it is possible to calculate the RMSD for this specific frequency range only. Therefore the variable n and the lower border of the sum in (1) have to be chosen accordingly.

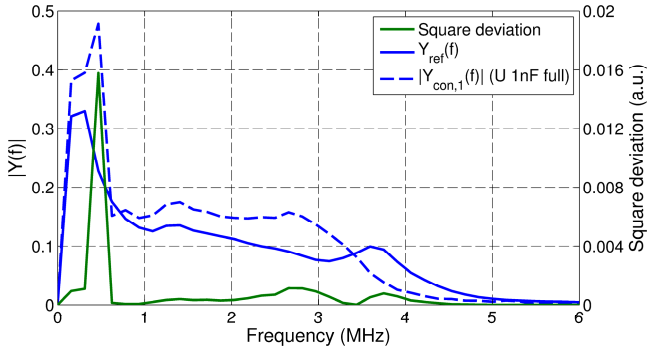

Fig. 4. Reference amplitude spectrum $Y_{ref}(f)$ (blue, solid trace), amplitude spectrum of one condition assessment $|Y_{con,1}(f)|$ (blue, dashed trace) for 1nF capacitor inserted in parallel to the full winding of phase U and calculated square deviation of both traces (green, solid trace).

The final Insulation State Indicator (ISI) is calculated according to (2) then. This indicator exists for each of the three phases.

$$ISI_p = \frac{\sum_{k=1}^{m} ISI_{p,k}}{m} \quad (2)$$

Linear combination of the three insulations state indicators can be used to calculate a Spatial Insulation State Indicator (SISI). The calculation of this indicator is performed according to (3).

$$SISI = ISI_U + ISI_V \cdot e^{j\frac{2\pi}{3}} + ISI_W \cdot e^{j\frac{4\pi}{3}} \quad (3)$$

The magnitude of this complex space phasor corresponds to the severity of change in the machine's high-frequency behavior. The angle determines the phase location. The linear combination has the additional effect that only asymmetrical changes are detected whereas symmetrical ones like due to temperature changes lead to a zero sequence component and are thus eliminated. Dirt effects influencing all three phases symmetrically do not influence the spatial insulation state indicator.

V. Experimental Setup

For proof of the proposed insulation condition monitoring technique experimental tests have been carried out on an

industrial 2-pole, 5.5kW squirrel-cage induction machine. Different windings of this machine are tapped and accessible at the machine terminal. Thus it is possible to realize short circuits without destruction of the machine. Furthermore it is possible to insert additional capacitances between the different taps. This alters the machine's high-frequency behavior by increasing e.g. the turn-to-turn capacitance $C_{t\text{-}t}$ as this additional fault C_{fault} capacitance is in parallel to $C_{t\text{-}t}$. To get a rough knowledge of the values of the involved parasitic capacitances the machine's phase-to-ground capacitance $C_{ph\text{-}gnd}$ and phase-to-phase $C_{ph\text{-}ph}$ were determined to 1.71nF and 742pF, respectively.

The measurements, control and signal processing are carried out with a combined system of Real-Time processor, Field Programmable Gate Array (FPGA) and fast sampling ADCs from National Instruments, programmable in LabVIEW.

VI. Experimental Results

The method's accuracy is strongly depending on the used sampling rate and bit resolution. The lower the necessary sampling rate and bit resolution can be the easier is the method to implement. All measurements were carried out with a sampling rate of 40MHz and 16bit resolution. The downsampling and signal processing is done offline.

A. Influence of Sampling Rate on Accuracy of ISI

As mentioned before to accurately detect changes in the machine's high-frequency behavior the transient oscillation with decaying magnitude visible in the phase current immediately after a switching transition has to be measured with sufficient resolution in time. As can be seen in Fig. 4 the most significant frequency component is in the range of 500kHz. According to the well known Nyquist theorem the minimum sampling rate needed to resolve this frequency is above 1MS/s. To show the performance of the condition monitoring technique for different sampling rates various scenarios have been realized. Cabling, shielding and grounding have been kept the same during all measurements. However, additional capacitors have been connected between different taps in different windings.

The sampling rate has been varied between 1MS/s and 40MS/s. To analyze the change of the statistical properties the mean value und standard deviation for the insulation state indicator of one phase ($ISI_{U,k}$) have been calculated. The indicators have been determined for various scenarios – for healthy machine condition and capacitors (200pF, 500pF and 1nF) added in parallel to the full and partial (~50%) phase winding U. For all sampling rates the variable n in equation (1) is chosen to 8 resulting in a frequency range from 0 to ~1MHz. The upper frequency limit f_{upper} can be calculated for a constant window length of 6.4µs and a sampling frequency f_S according to (4).

$$f_{upper} = \frac{(n-1)\cdot f_S}{N};\ N = 6.4\mu s \cdot f_S;\ n = 1,2,3,... \qquad (4)$$

Investigations have shown that the changes in the machine's high-frequency behavior due to alteration of the winding capacitance affect the frequency component around 500kHz. Change of cabling on the other side leads to a change at a higher frequency component (around 1.7MHz). Thus the chosen frequency range only takes into account the winding insulation state induced alterations. The results of this analysis can be seen in Fig. 5 with (a) showing the standard deviation and (b) the mean value. A clear trend can be detected that – as one would expect – the standard deviation increases with decreasing sampling rate. For the different investigated scenarios the standard deviation is in a narrow range for constant sampling rate. A reduction of the sampling rate to 20MS/s is hardly affecting the quality of the insulation state indicator.

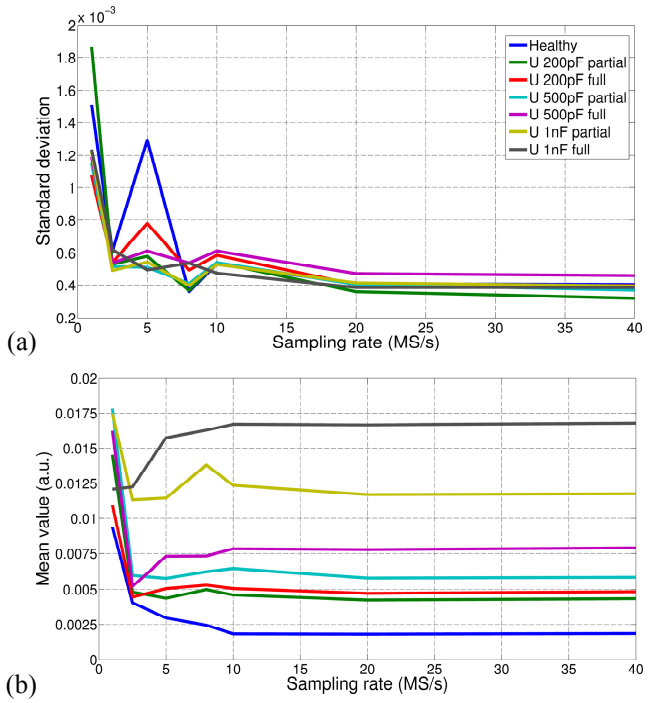

Fig. 5. (a) Standard deviation and (b) mean value for different investigated scenarios in dependency of sampling rate.

However, evaluation of indicator's quality can only be done if the mean value in addition to the standard deviation is taken into account. Table I summarizes the standard deviation and mean value of the insulation state indicator for different scenarios and sampling rates (5, 10 and 40MS/s).

TABLE I. Comparison of Mean Value and Standard Deviation for Different Sampling Rates and Scenarios.

Scenario	$ISI_{U,k}$; k=1…140					
	Mean value (·10^{-3})			*Standard deviation(·10^{-3})*		
Sampling rate (MS/s)	5	10	40	5	10	40
Healthy	3	1.8	1.9	1.3	0.53	0.40
U 200pF partial	4.4	4.6	4.3	0.58	0.54	0.32
U 200pF full	5.1	5.1	4.8	0.78	0.59	0.40
U 500pF partial	5.8	6.5	5.9	0.51	0.54	0.37
U 500pF full	7.3	7.8	7.9	0.61	0.61	0.46
U 1nF partial	11.5	12.4	11.8	0.54	0.53	0.39
U 1nF full	15.8	16.7	16.8	0.49	0.47	0.38

The mean values and thus the later used insulation state indicators ISI_U (see equation (3)) for all scenarios and sampling rates are in the same range of magnitude. However, the standard deviation clearly increases with decreasing sampling

rate. This makes it more difficult to separate the different scenarios. Thus the smallest detectable alteration of the machine's high-frequency behavior increases.

Based on these results it can be concluded that an accurate monitoring of the insulation state is possible with a sampling rate 10-times higher than the interesting frequency (in the investigated case this frequency is around 500kHz; see Fig. 4). However, the sensitivity is reduced. A recommendation of the authors is a sampling rate of 20-times higher than the interesting frequency for high performance.

B. Influence of Bit Resolution on Accuracy of ISI

Another important parameter regarding the sampling of data that significantly influences the accuracy of the proposed condition monitoring technique is bit resolution. The influence of this parameter is analyzed in this chapter. The sampling rate is kept constant at 40MS/s for all investigations in this section. Again different scenarios are evaluated and the influence of reduced bit resolution on the quality of the insulation state indicator $ISI_{U,k}$ for each measurement is analyzed. Fig. 6 shows the (a) standard deviation (b) and mean value for various scenarios over different resolution between 6 and 16bit.

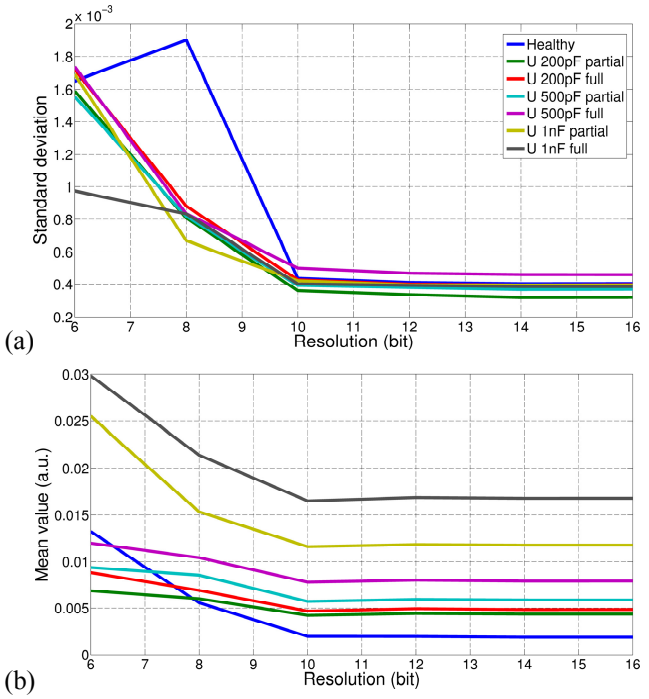

Fig. 6. (a) Standard deviation and (b) mean value for different investigated scenarios in dependency of bit resolution.

The results clearly show that a reduction of the resolution from 16bit to 10bit hardly affects the quality of the insulation state indicator. However, a further reduction leads to a distinct decrease of indicator quality. Table II again summarizes the results for mean value and standard deviation of the insulation state indicator for different scenarios.

The results clearly show that a reduction of the resolution to 10bit hardly affects the indicator quality. However, resolution should not be lower than 10bit as the insulation state indicator ISI_U (mean value of $ISI_{U,k}$) significantly differs from the one with 16bit and the standard deviation is significantly increased. Thus the authors recommend a resolution of at least 10bit.

TABLE II. COMPARISON OF MEAN VALUE AND STANDARD DEVIATION FOR DIFFERENT BIT RESOLUTION AND SCENARIOS.

Scenario	$ISI_{U,k}$; k=1…140					
	Mean value ($\cdot 10^{-3}$)			*Standard deviation($\cdot 10^{-3}$)*		
Resolution (bit)	8	10	16	8	10	16
Healthy	5.6	2.0	1.9	1.9	0.44	0.40
U 200pF partial	6.0	4.2	4.3	0.81	0.36	0.32
U 200pF full	6.9	4.7	4.8	0.88	0.43	0.40
U 500pF partial	8.5	5.7	5.9	0.82	0.39	0.37
U 500pF full	10.4	7.8	7.9	0.84	0.50	0.46
U 1nF partial	15.3	11.6	11.8	0.67	0.42	0.39
U 1nF full	21.4	16.5	16.8	0.83	0.40	0.38

C. Comparison of optimum and recommended minimum sampling parameters

The maximum tested sampling rate was 40MS/s. The best results may be obtained with higher sampling rates. However, indicator quality will increase only slightly.

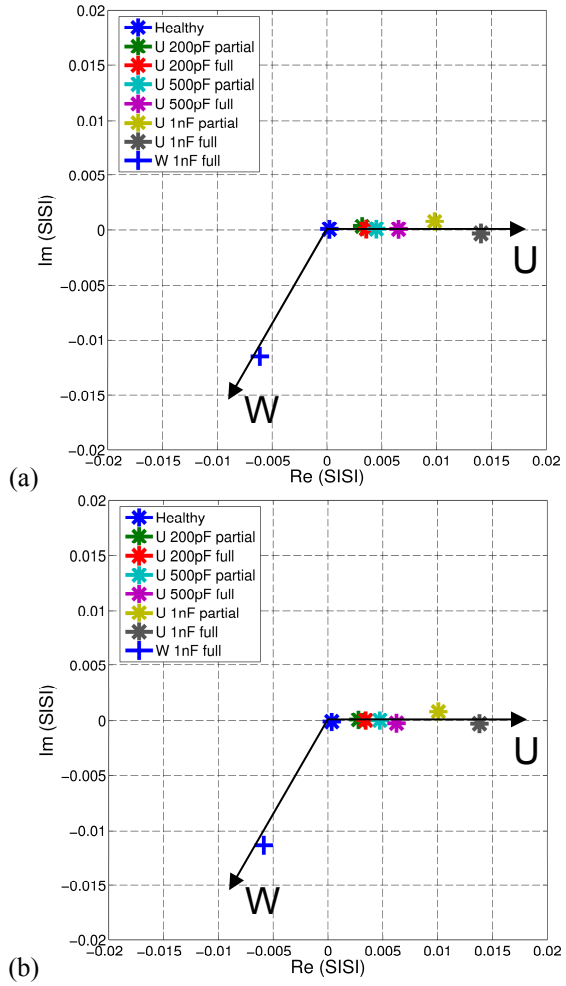

Fig. 7. Spatial insulation state indicator (SISI) for different investigated machine conditions; (a) sampling rate: 40MS/s resolution: 16bit, (b) sampling rate: 10MS/s resolution: 10bit.

Thus the maximum parameters for the sampling of the current signal are a sampling rate of 40MS/s and a resolution of 16bit in this investigation. The recommended minimum setting is a sampling rate of 10MS/s (factor of 20 above interesting

frequency) and a resolution of 10bit. In Fig. 7 the spatial insulation state indicator (SISI) is depicted for different investigated scenarios. Different capacitors have been inserted in parallel to the full and partial (~50%) phase winding of phase U and W. Furthermore Fig. 7 clearly shows that for both parameter sets (a) 40MS/s, 16bit; (b) 10MS/s, 10bit the results are very similar. The spatial insulation state indicators for all scenarios correlate in magnitude and angle. Therefore a separation of the different scenarios in severity and location is possible. The angle of the spatial insulation gives the information of the phase location of insulation degradation. To better show this correlation the obtained spatial insulation state indicators for the different investigated scenarios are summarized in Table III in magnitude and angle. A good correlation could be found. Thus the quality of the indicator is high for both investigated sampling parameter sets.

TABLE III. SPATIAL INSULATION STATE INDICATORS SISI GAINED AT DIFFERENT MACHINE CONDITIONS FOR DIFFERENT SAMPLING PARAMETERS.

Scenario	***SISI***			
	Optimum 40MS/s 16bit		***Minimum recommended 10MS/s 10bit***	
	Magnitude ($\cdot 10^{-4}$)	Angle	Magnitude ($\cdot 10^{-4}$)	Angle
Healthy	2.33	---	3.53	---
U 200pF partial	32.29	5.94°	27.81	1.97°
U 200pF full	35.84	1.71°	34.39	0.66°
U 500pF partial	45.04	1.27°	47.29	0.44°
U 500pF full	65.32	0.79°	62.56	-2.13°
U 1nF partial	98.84	4.48°	100.97	4.66°
U 1nF full	140.45	-1.24°	138.19	-1.14°
W 1nF full	130.40	-118.02°	128.51	-117.35°

VII. CONCLUSIONS

A condition monitoring technique capable of detecting changes in the machine's high-frequency behavior has been presented. The method evaluates the current's reaction on a change of the switching state by the voltage source inverter. Due to the mismatch of cable and machine impedance and the high rate of voltage rise the applied voltage pulse is reflected at the machine terminal. This leads to a decaying high-frequency oscillation visible in the voltage and current signal. The characteristic of this oscillation is determined by the machine's high-frequency behavior. The capacitances e.g. due to the machine's or cable's insulation system significantly influence this hf-behavior. If the insulation system ages over time, this degradation changes these capacitances and thus the machine's hf-behavior. These changes are detectable by analyzing the characteristic parameters of the hf-oscillation in the measured phase current. The characteristic used in this investigation is the amplitude spectrum of the current oscillation. A comparison of the amplitude spectrum of a condition measurement to a previously stored amplitude spectrum for the healthy machine allows defining an insulation state indicator. The used comparative value is the root mean square deviation. The parameters of the sampling significantly influence the accuracy of the proposed technique. Changes in the machine's insulation capacitance result in a change in a certain frequency range in the amplitude spectrum. The analysis shows that very good results can be achieved if the sampling rate is about 20 times higher than this interesting frequency. However, satisfying results can still be achieved with a sampling rate of 10 times higher than the interesting frequency. Concerning the bit resolution 10bit are enough to achieve very good results. This resolution is easily met in modern drive systems.

It has been proven that with these recommended parameters a change in the machine's hf-behavior can be detected with high sensitivity in severity and phase location.

ACKNOWLEDGMENT

The work to this investigation was supported by the Austrian Science Fund (FWF) under grant number P23496-N24. The authors want to thank National Instruments Austria and especially DI Günther Stefan for the generous support and donation to finance the measurement hardware.

REFERENCES

[1] IEEE Committee Report; "Report of large motor reliability survey of industrial and commercial installation, Part I," *IEEE Transactions on Industry Applications,* vol.21, no.4, pp.853–864, 1985.

[2] IEEE Committee Report; "Report of large motor reliability survey of industrial and commercial installation, Part II," *IEEE Transactions on Industry Applications,* vol.21, no.4, pp.865–872, 1985.

[3] Kim, H.D.; Yang, J; Cho, J.; Lee, S.B.; Yoo, J.-Y.; "An Advanced Stator Winding Insulation Quality Assessment Technique for Inverter-Fed Machines," *IEEE Trans. on Ind. Appl.,* vol.44, no.2, pp.555-564, 2008.

[4] Grubic, S.; Aller, J.M.; Bin Lu; Habetler, T.G.; "A Survey on Testing and Monitoring Methods for Stator Insulation Systems of Low-Voltage Induction Machines Focusing on Turn Insulation Problems," *IEEE Trans. on Industrial Electronics,* vol.55, no.12, pp.4127-4136, 2008.

[5] Schump, D.E.; "Testing to assure reliable operation of electric motors," *Industry Applications Society 37th Annual Petroleum and Chemical Industry Conference,* pp.179-184, 1990.

[6] Stone, G.C.; "Recent important changes in IEEE motor and generator winding insulation diagnostic testing standards," *IEEE Transactions on Industry Applications,* vol.41, no.1, pp. 91- 100, 2005.

[7] Stone, G.C.; Boulter, E.A.; Culbert, I. and Dhirani, H.; "Electrical insulation for rotating machines – Design, Evaluation, Aging, Testing, and Repair," IEEE Press, John Wiley & Sons, 2004.

[8] Wiedenbrug, E.; Frey, G.; Wilson, J.; "Impulse testing and turn insulation deterioration in electric motors," *Annual Pulp and Paper Industry Technical Conference,* pp. 50- 55, 2003.

[9] Stone, G.C.; Sedding, H.G.; Costello, M.J.; "Application of partial discharge testing to motor and generator stator winding maintenance," *IEEE Trans. on Industry Applications,* vol.32, no.2, pp.459-464, 1996.

[10] Joksimovic, G.M.; Penman, J.; "The detection of inter-turn short circuits in the stator windings of operating motors," *IEEE Transactions on Industrial Electronics,* vol.47, no.5, pp.1078-1084, 2000.

[11] Nandi, S.; Toliyat, H.A.; "Novel frequency-domain-based technique to detect stator interturn faults in induction machines using stator-induced voltages after switch-off," *IEEE Trans. on Ind. Appl.,* vol.38, no.1, pp.101-109, 2002.

[12] Grubic, S.; Habetler, T.G.; Restrepo, J.; "A new concept for online surge testing for the detection of winding insulation deterioration," *Energy Conversion Congress and Exposition (ECCE),* pp.2747-2754, 2010.

[13] Peroutka, Z.; "Requirements for insulation system of motors fed by modern voltage source converters," *IEEE 35th Annual Power Electronics Specialists Conference, PESC,* vol.6, pp. 4383- 4389, 2004.

[14] Wolbank, T.M.; Wohrnschimmel, R.; "Transient electrical current response evaluation in order to detect stator winding interturn faults of inverter fed ac drives," *Symposium on Diagnostics for Electric Machines, Power Electronics and Drives (SDEMPED),* pp.1-6, 2001.

[15] Perisse, F.; Werynski, P.; Roger, D.; "A New Method for AC Machine Turn Insulation Diagnostic Based on High Frequency Resonances," *IEEE Trans. on Diel. and El. Ins.,* vol.14, no.5, pp.1308-1315, 2007.